sustainability

MDPI

Article

The Impact of Climate Variability on the Blooming of *Fraxinus ornus* 'Globosa' as a Component of Novi Sad's (Serbia) Green Infrastructure

Jelena Čukanović [1], Mirjana Ljubojević [1], Sara Djordjević [1], Tijana Narandžić [1], Djurdja Petrov [2] and Mirjana Ocokoljić [2,*]

[1] Faculty of Agriculture, University of Novi Sad, Trg Dositeja Obradovića 8, 21000 Novi Sad, Serbia; jelena.cukanovic@polj.uns.ac.rs (J.Č.); mirjana.ljubojevic@polj.uns.ac.rs (M.L.); sara.djordjevic@polj.edu.rs (S.D.)
[2] Faculty of Forestry, University of Belgrade, Kneza Viseslava 1, 11030 Belgrade, Serbia; djurdja.stojicic@sfb.bg.ac.rs
* Correspondence: mirjana.ocokoljic@sfb.bg.ac.rs

Abstract: Climate change increasingly impacts urban dendroflora, affecting plant physiology and phenological phases. This paper investigates the impact of changing climatic conditions on the blooming of *Fraxinus ornus* 'Globosa', a decorative form of ash that is a significant component of green infrastructure in Novi Sad, Serbia. The research, conducted over 15 years on 42 individuals in a linear planting near a large river, analyzed temperature and precipitation effects on blooming times and inflorescence characteristics The results indicate changes in the timing of blooming, earlier than recorded in the literature, suggesting that temperature variations and changes in climatic conditions have significantly influenced the phenological phases of the selected clones of globe flowering ash. Additionally, the studied individuals showed exceptional adaptation to climate change and are not considered vulnerable. This study confirmed that this cultivar of flowering ash in urban environments is a key link in the green infrastructure of cities, functioning as green corridors along river flows as a nature-based solution. The studied cultivar is an important element of cultural heritage, contributing to the recreational potential of the linear composition of the promenade, especially during the flowering phenophase, when, in addition to its aesthetic values, it has psychological effects on users of the space, offering a calming influence due to its regular canopy and planting rhythm. Additionally, this cultivar provides important ecological functions, such as offering pollen for pollinators, thereby significantly contributing to the implementation of ecosystem services.

Keywords: globe flowering ash; flowering time; inflorescence morphology; climate changes; green infrastructure; landscape architecture

Citation: Čukanović, J.; Ljubojević, M.; Djordjević, S.; Narandžić, T.; Petrov, D.; Ocokoljić, M. The Impact of Climate Variability on the Blooming of *Fraxinus ornus* 'Globosa' as a Component of Novi Sad's (Serbia) Green Infrastructure. *Sustainability* **2024**, *16*, 8404. https://doi.org/10.3390/su16198404

Academic Editor: Richard Ross Shaker

Received: 20 August 2024
Revised: 20 September 2024
Accepted: 24 September 2024
Published: 27 September 2024

1. Introduction

Cities are threatened by intensified urbanization and global climate changes, which lead to rising air temperatures and the effects of urban heat islands (UHI) [1]. In this context, elements of green infrastructure (GI), as parts of cultural ecosystems (parks, residential blocks, green corridors along roads and rivers, private gardens, and other elements of special purpose), play an important role in both suburban and central zones of urban areas [2]. The ecological benefits of GI are significant for the health, protection, promotion, and preservation of biodiversity, and they are also a means for mitigating and improving microclimatic conditions in urban environments [3]. In particular, trees—as an element of GI—provide cities with benefits such as managing atmospheric runoff, improving air quality, accumulating carbon, providing shade, reducing UHI effects, and being a crucial link in biodiversity [4]. As a key ecosystem service related to biodiversity, the interdependence between woody plants and insects, and vice versa, stands out [5]. Additionally, the

presence of trees contributes to the ornamental value and character of the urban landscape by influencing aesthetics and visual perception [6,7]. Flower-decorative woody species represent an important element of GI in cities. Research into flowers and blooming can provide valuable data on plant adaptability. Phenological observations in Japan, through the analysis of very long data series, indicate the effects of climate change on ornamental woody plants [8]. It has been established that urbanization, temperature variations, warming, and urban heat islands also affect the shifting of flowering phenophases. According to Kunz and Blanke [9], the strongest correlations occur between air temperature and the beginning of flowering phenophases.

Within the *Oleaceae* family and genus *Fraxinus*, since it was described by Linnaeus in 1753, 800 different taxa have been classified, including species, subspecies, and varieties. The genus *Fraxinus* Tourn. ex L. is widely distributed across the northern hemisphere, from tropical to temperate climate zones. It predominantly includes tall and medium-tall trees, with a small number of shrub species found in arid regions. *Fraxinus* contains both wind- and insect-pollinated species, and the breeding systems range from hermaphrodites through androdioecious and polygamous to dioecious species [10]. It is divided into several sections, and the species manna ash (*Fraxinus ornus* L.) belongs to the section Ornus, which is characterized by inflorescences on one-year-old twigs. The manna ash belongs to the group of ashes with petal-like structures, and this morphological characteristic justifies its name "flowering ash" and places it in the group of ornamental ash species. As a basic species, it has been used less frequently in urban green spaces in recent decades, but due to its exceptional characteristics, the cultivar of manna ash with a globular crown shape, *Fraxinus ornus* 'Globosa' (H.A. Hesse (Nurs.)), is more commonly used.

Given the above, the focus of the work is on the phenological patterns and key blooming events of *Fraxinus ornus* 'Globosa' (H.A. Hesse (Nurs.)), synthesized in 1933 in Germany [11], under the conditions of climate change, within the GI of Novi Sad. The research is based on the importance, and definition of ecological protection measures, conservation of *Fraxinus ornus* 'Globosa', and the benefits for the population, ecosystem services, and the sustainability of linear greenery near a major river flow in the compact urban core with the aim of: (1) determining the status and prospects for the application of globe flowering ash in GI, (2) the impact of climate change on linear planting by comparing phenological blooming patterns and climatic elements, and (3) determining the sex of selected trees and the morphometric characteristics of inflorescences as they contribute to the visual perception of the urban landscape.

2. Materials and Methods

2.1. Study Area

The research area is a linear planting of *Fraxinus ornus* 'Globosa', from the coordinates 45°15′39.24″ N; 19°51′23.44″ E at an altitude of 74 m to the coordinates 45°15′02.15″ N; 19°51′21.75″ E at an altitude of 76 m, within the green infrastructure of Novi Sad (Figure 1) in Serbia, in southeastern Europe. The total length of the reconstructed quay in 2010, where 42 globe flowering ash trees were planted along the cycling and pedestrian path (with an average slope of 3°), is 1184.06 m. The research area is located on the left bank of the Danube in the Bačka part of the city, while on the right bank begins the territory of Srem with a different spatial arrangement of elements and relief (Figure 1).

The area of the Bačka part of Novi Sad is located on a uniform geological substrate in a region with minimal relief variation, consisting of alluvial (fluvisol) and deluvial (colluvium) soils [12]. According to the pedological map of Vojvodina [13], the research area features alluvial sandy soil. The soil of the studied quay is anthropogenized and is typical of urbisol [12]. The quay is situated in an area where the natural potential vegetation would be fresh willow and poplar (*Salicion albae* Soo) [14].

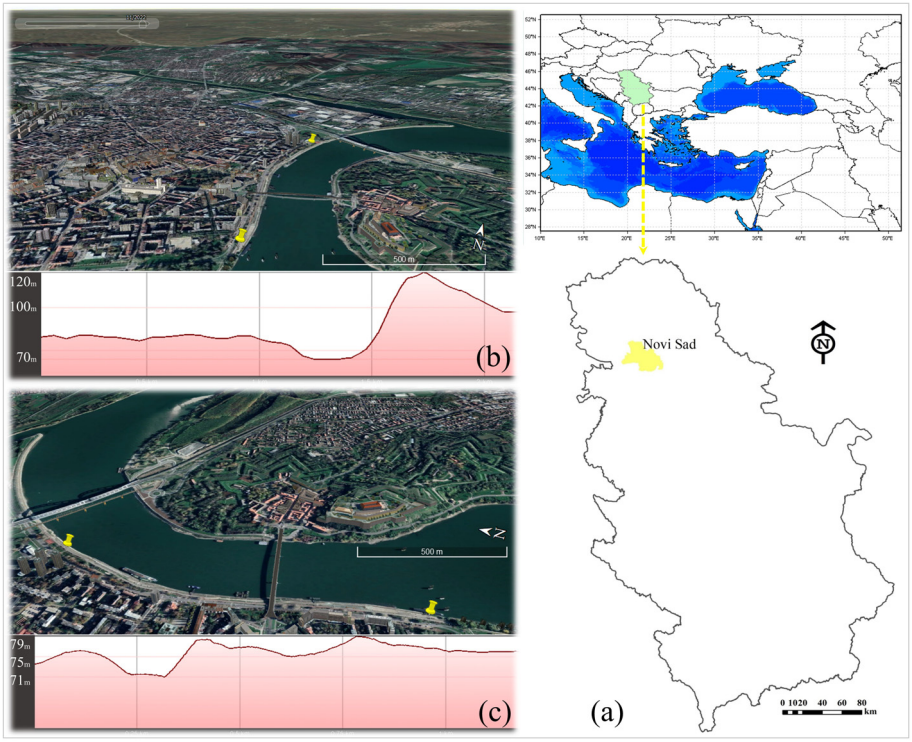

Figure 1. The location of Novi Sad in Europe and Serbia (**a**), research area with profiles: (**b**) Bačka (left bank) and Srem (right bank) territories of Novi Sad (view: south–southwest (SSW)—north–northeast (NNE)), and (**c**) the studied part of the quay on the left bank of the Danube (view from west-northwest—WNW).

2.2. Acquisition of Data

2.2.1. Climatic Data

According to WMO [15] recommendations for deviations in climatic parameters, data for the reference period (1991–2020) and the research period (2010–2023), as well as older time series 1961–1991, 1971–2001, 1981–2011, and the first five months of 2024, were obtained from the Republic Hydrometeorological Institute of Serbia (RHMZ) [16,17] from the main meteorological station (MMS) Rimski Šančevi (45°19′19.97″ N; 19°49′48.01″ E; altitude: 86 m). Considering the distance of Rimski Šančevi from the research area, data interpolation from 28 MMS RHMZ stations was performed using the method by Fries et al. [18] to validate the relevance of the climatic parameters. Climatic parameter normals were determined, particularly the average air temperatures by periods and seasons, as well as for February, March, April, and May for the reference period (1991–2020) and the research period. Statistical climatological methods of percentiles and corresponding terciles were also applied, where the n-th percentile is the value below which n percent of data falls when sorted in ascending order (RHMZ).

2.2.2. Phenological Data

The phenological data result from intensive phenological monitoring of the blooming of 42 globe flowering ash trees from the establishment of the planting (2010) to the present day (2024). The research was conducted over 15 consecutive years. Phenological monitoring was carried out visually every other day on all plants. A system of digital messages was used, which were converted into days of the year (DOYs) according to Koch et al. [19] via software, where DOY 1 represents January 1, and so on. For uniform coding of blooming phenophases, the extended general BBCH scale [20] and the percentage of open flowers [21] were used, where: BF indicates the beginning of flowering (the day when more than 10% of flowers on most of the canopy or a larger number of inflorescences are open), FF indicates

full flowering (the day when more than 50% of flowers are open), and EF indicates the end of flowering (the day when fewer than 20% of inflorescences are present).

2.2.3. Plant Material

Inflorescences were sampled at the full flowering stage in 2024 from the southern part of the canopy of the linearly planted individuals (Figure 2) of the globe-shaped cultivar of manna ash, *Fraxinus ornus* 'Globosa' (H.A. Hesse (Nurs.)).

(**a**) (**b**)

Figure 2. Flowering globe ash in the full flowering (**a**) and full leafing stage (**b**) in Novi Sad (Serbia).

Morphometric analysis and determination of flower sex were performed on a sample of 420 inflorescences (10 inflorescences from each individual). The analysis was conducted using the UTHSCSA Image Tool program (Figure 3), examining the following parameters: inflorescence length (IL), inflorescence width (IW), number of flower clusters (NFC), number of pistils in a single flower (NP), and number of stamens (NS).

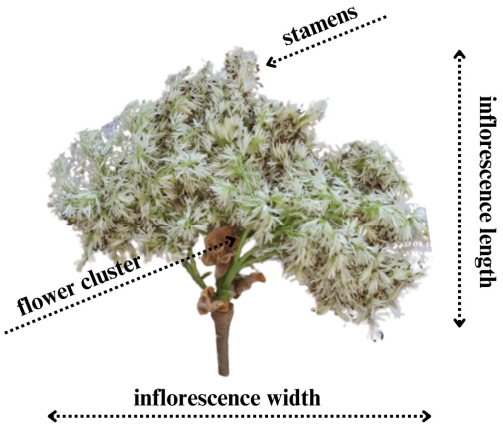

Figure 3. Measured parameters on the sampled inflorescence of flowering ash.

The sex of the individuals was determined visually and then verified microscopically using a Motic Digital BA310 biological light microscope with a built-in digital camera. Images of cross-sections were taken at 40× and 400× magnifications, and measurements

were performed using the image analyzing system Motic Images Plus 2.0; Motic China Group Co., etc.

2.3. Processing of Data

Given that phenophases do not occur according to dates but after the accumulation of heat [22], the method of determining growing degree days (GDD) was applied, using the maximum (T_{max}) and minimum (T_{min}) daily air temperatures and the temperature threshold (Tt). In the study for Novi Sad, a T_t of 5 °C was used according to WMO recommendations [23] for temperate continental climate conditions. GDD was determined according to the method of McMaster and Willhelm [24], supplemented by the method of Lalić et al. [22]. For globe flowering ash, the heat requirements for key events in the blooming phenological pattern were determined by combining phenological and climatological data: BF, FF, and EF. Active temperature sums were accumulated from January 1 for each day until BF, FF, and EF in 2010. The procedure was repeated for each subsequent year until 2024.

The study employed descriptive statistics, the Spearman rank test (ρ), the non-parametric Mann–Kendall trend test according to Gilbert [25], the Duncan multiple range test, analysis of variance (ANOVA), and cluster analysis dendrogram (Cluster). The Spearman rank test was chosen due to its broader significance than the linear correlation coefficient, showing whether there is a consistently increasing or decreasing relationship between variables. It also does not require an assumption about the frequency distribution of variables, and the value and sign (ρ from −1 to 1) determine the strength and direction of the relationship. Only significant correlations with a probability of $p < 0.05$ were analyzed.

For data processing, the software packages XLSTAT 2020, The STATISTICA 13 (TIBCO Software Inc., Palo Alto, CA, USA, 2020), Past 4.11, ArcGIS 10.8/ArcMap 10.8, and Google Earth Pro 7.1.8 for Windows were used.

3. Results

3.1. Chronology of Climatic Parameters

Given that the focus of the work is on climate change based on the parameters from MMS Rimski Šančevi, which is 7038.6 m away in a straight line from the NNE (north–northeast) point of the research area, the spatial distribution of average daily air temperatures (normals) by seasons for the research period 2010–2023, winter and spring 2024, and the months of February, March, April, and May for the periods 2010–2023 and 2024 were determined using interpolation (Figures 4–6). The term "normal" refers to the climatological standard normal, i.e., the average value of a climatic parameter (in this case, air temperature) calculated for the period from 1 January 2010 to 31 December 2023, and the mentioned months (average values for February, March, April, and May in the period 2010–2024), as well as for the reference period from 1 January 1991 to 31 December 2020. The adequacy of the air temperatures used to determine GDD is confirmed with a precision of 0.1 °C, as evident in Figures 4–6, where it can be observed that Rimski Šančevi and the research area belong to the same temperature range.

The average seasonal air temperature during winter in the period 2010–2023 was 2.5 °C to 2.6 °C, while during the winter of 2024, it ranged from 5.8 °C to 5.9 °C (Figure 4). The previous maximum average seasonal temperature for the historical period 1949–2023 was recorded in 2007 (4.9 °C), a year outside the research period. During the winter of 2024, there was also a record of the highest average maximum temperatures (11.0 °C) and the highest average minimum air temperatures (1.7 °C) in the same historical period according to RHMZ [26]. During the winter of 2024, there were no cold waves (continuous periods of five or more days when the minimum daily air temperature falls within the very cold and extremely cold range), but there were two heat waves (periods of five or more days when the maximum daily air temperature falls within the very warm and extremely warm range) lasting 11 days (late December and early January) and 8 days (in the first and early second decade of February).

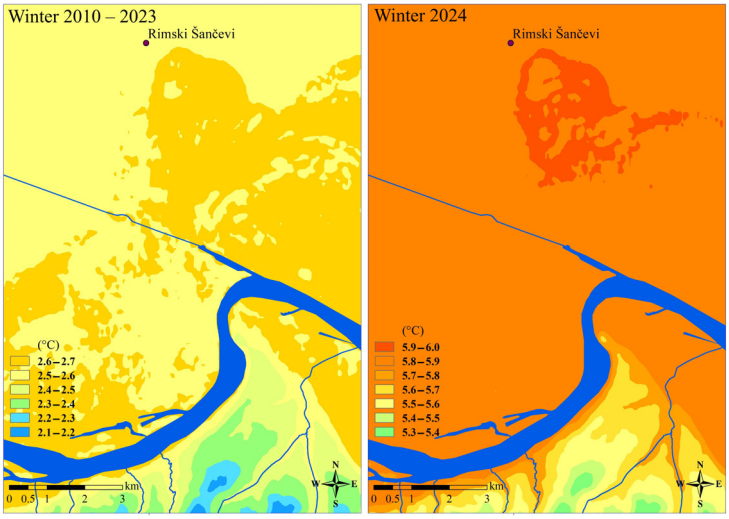

Figure 4. Spatial distribution of average winter air temperatures (normals) in (°C) for the periods 2010–2023 and 2024, based on RHMZ data.

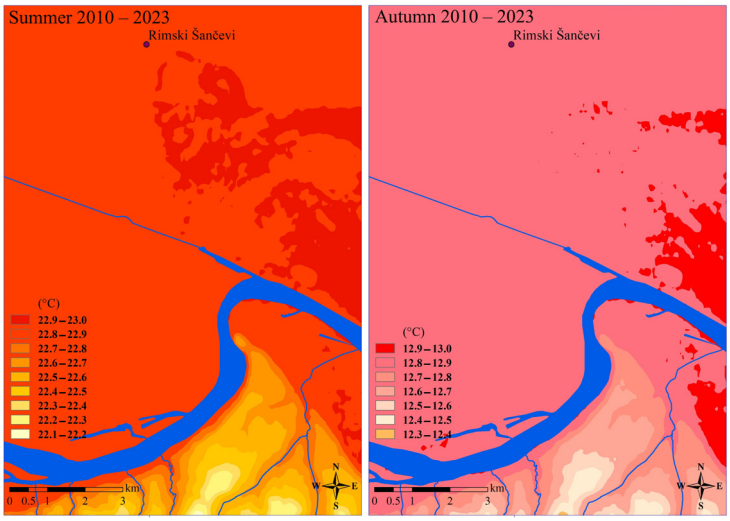

Figure 5. Spatial distribution of average summer and autumn air temperatures (normals) in (°C) for the period 2010–2023, based on RHMZ data.

The average seasonal air temperature during spring in the period 2010–2023 was 12.4 °C to 12.5 °C, while during the spring of 2024 it ranged from 15.2 °C to 15.3 °C. During the spring of 2024, there were no cold waves, but two heat waves lasted 5 days (late March and early April) and 12 days (in the second half of the first decade to the middle of the second decade of April). For the historical period 1949–2023, the maximum average seasonal temperature of 2024, which was 15.3 °C, surpassed the previous maximum recorded in 2018 (14.2 °C). During the spring of 2024, there was also a record of the highest average maximum temperatures (21.7 °C), with the previous maximum being 2018 (19.9 °C), as well as the highest average minimum air temperatures (8.8 °C), with the previous maximum average minimum temperature also recorded in 2018 (8.6 °C) in the same historical period according to RHMZ [27].

The average seasonal air temperature during summer in the period 2010–2023 was 22.8 °C to 22.9 °C, and during autumn, it ranged from 12.8 °C to 12.9 °C (Figure 5). In the fourteen-year consecutive research period, the year 2023 stands out, as the average summer air temperature deviated the most (by 1.4 °C) from the normal of the reference period 1991–2020 [28]. During autumn, there was a record of 12 tropical days (days with a maximum air temperature of 30 °C and above) and 40 summer days (days with a maximum

daily air temperature of 25 °C and above), and the average autumn air temperature deviated by +3.4 °C compared to the normal of 1991–2020 [29].

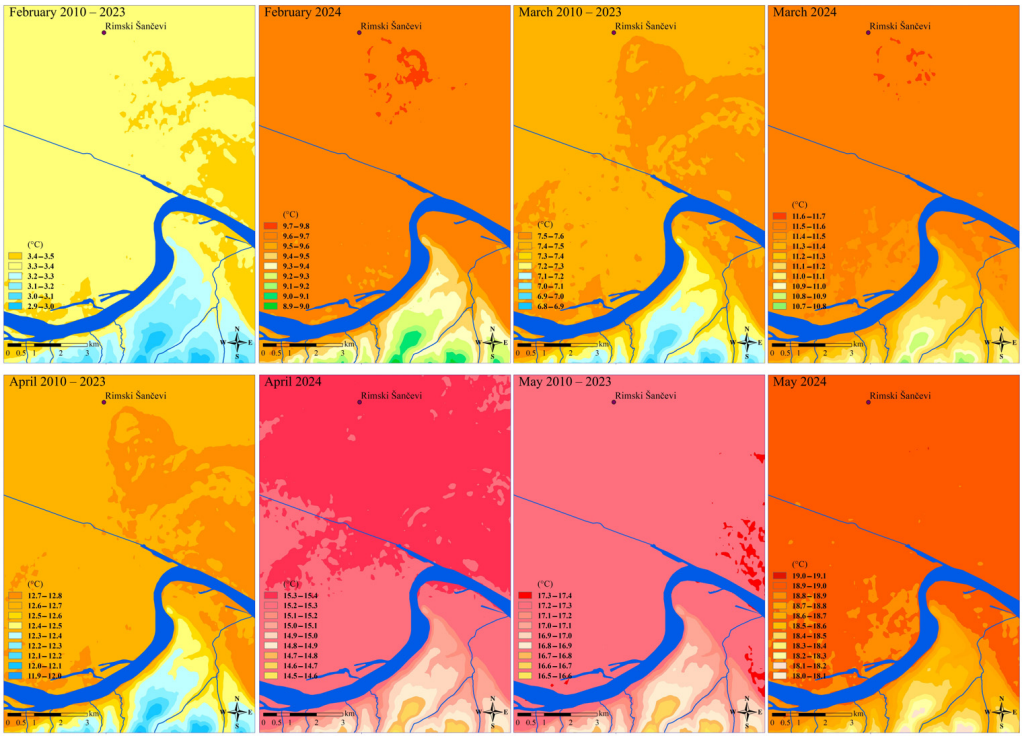

Figure 6. Spatial distribution of average monthly air temperatures (normals) for February, March, April, and May in (°C) for the periods 2010–2023 and 2024, based on RHMZ data.

During the months when the globe flowering ash underwent its flowering phenophase, the mean monthly air temperatures for the period 2010–2023 were as follows: February 3.3 °C to 3.4 °C, March 7.4 °C to 7.5 °C, April 12.7 °C to 12.8 °C, and May 17.2 °C to 17.3 °C. In 2024, significant deviations were recorded compared to the first 14 years of research: February was the warmest and driest, with the lowest number of frost days in the history of measurements, and mean air temperatures were 9.7 °C to 9.8 °C; March was the warmest, with average rainfall and temperatures of 11.5 °C to 11.6 °C; April was the fourth warmest, with the maximum daily temperature surpassed on 15 April, while mean temperatures were 15.3 °C to 15.4 °C; May was averagely warm, with precipitation around and slightly above normal, and mean temperatures of 18.9 °C to 19.0 °C (Figure 6). The maximum average monthly temperatures for the historical period 1949–2023 were for February 2016 (7.5 °C), March 2001 (10.2 °C), April 2018 (17.2 °C), and May 2003 (20.6 °C). In 2024, there was also a record of the highest average maximum temperatures for February (15.7°C) and March (17.6°C), with the previous maximums being for February 1990 (12.9°C), March 2019 (16.7°C), April 2018 (23.7°C), and May 2003 (27.5°C). The maximum average of minimum air temperatures for 2024 was exceeded in February (4.8°C) and March (5.6°C), with the previous maximums being for February 2016 (2.9°C), March 2001 (5.3°C), April 2018 (10.7°C), and May 2018 (14.3°C) in the same historical period according to RHMZ. During February, March, April, and May 2024, there were no cold waves, while heat waves were recorded in February (4.2–11.2), March, and April (29.3–2.4 and 5.4–16.4).

The average values and sums, average monthly air temperature, average maximum air temperature, average monthly minimum air temperature, average and monthly precipitation amounts, average and monthly sunshine duration, the average and number of days with precipitation $\geq$ 0.1 mm, and the average and number of days with precipitation $\geq$ 1.0 mm were calculated on a monthly and annual basis for the reference period, the research period, and older time series (Table S1).

A comparative analysis of the mean annual air temperatures reveals an upward trend (Table S1). The mean annual air temperature during the reference period in Novi Sad shows an increase compared to older time series by 0.5 °C to 1.0 °C, and during the research period, from 0.8 °C to 1.6 °C. The year 2023 stands out as the hottest year in Novi Sad. The rising temperature trend continued/will continue throughout 2024. During the months when the globe flowering ash underwent its flowering phenophase, mean temperatures were higher by 7.4 °C in February, 4.5 °C in March, 2.9 °C in April, and 1.6 °C in May. An increase in mean maximum temperatures was recorded: 8.8 °C in February, 4.9 °C in March, 4.1 °C in April, and 1.8 °C in May, as well as minimum temperatures of 6.5 °C in February, 3.7 °C in March, 1.4 °C in April, and 1.5 °C in May. The specific conditions of 2024 are also reflected in the increase in the number of summer days, with 2 recorded in March and 13 in April, along with one tropical day in April. There were no frost days in March, April, or May, and the number of frost days decreased by 15.8 in February and by 8.6 in March. For the first time compared to all earlier time series, the reference and research periods, no frost days were recorded in April 2024. The results of the comparative analysis of air temperatures align with the IPCC's [30] statement that warming is greater over land in many regions and exceeds the global annual average. In fact, the IPCC [31] stated that global warming between 2030 and 2052 would reach 1.5 °C, which was surpassed in the period from 2010 to 2023 in Novi Sad. The annual precipitation during the research period (2010–2023) was lower by 0.8 mm to 99.9 mm. A significant precipitation deficit was recorded during 2024, expressed as a percentage deviation in the total precipitation: 25.0% in February, 38.8% in March, 46.1% in April, and 78.9% in May. A notable decrease in the number of days with precipitation $\geq$ 1.0 mm is highlighted, ranging from 0.7 to 1.4 days for the period 2010–2023 compared to the reference period and older time series. The year 2024 stands out, with the number of days with precipitation $\geq$ 1.0 mm being lower by 3.5 in March and 4 in April. The mean monthly sunshine duration increased by 52.1 h to 236.4 h during the research period. During the months of the flowering phenophase in 2024, the number of sunshine hours was higher compared to all previous periods shown in Table S1: by 42.1 h in February, 26.3 h in March, 100.7 h in April, and 50.7 h in May. The presented results of average monthly air temperatures (°C) and precipitation sums (mm) categorized through percentiles and terciles are shown in Tables 1 and 2 for the first five months of 2024. In February and March, it was extremely warm (percentiles) or warm (terciles) and dry, in April very warm and dry, while May was warm with precipitation in the normal category.

Table 1. Average monthly air temperatures and corresponding percentiles and terciles and their deviations for February, March, April, and May 2024, in Novi Sad (Serbia), compared to the reference period 1991–2020.

T_{mean} (°C)	Perc. Cat. *	T_{mean} (°C)	Deviation (°C)	1991–2020	1991–2020	1991–2020	Terciles **
	1991–2020	1991–2020		33.-Perc.	50.-Perc.	66.-Perc.	Cat.
February							
9.7	EW	2.3	7.4	1.9	2.9	4.1	1
March							
11.5	EW	7.0	4.5	5.9	6.8	7.9	1
April							
15.3	VW	12.4	2.9	11.8	12.6	13.1	1
May							
18.9	W	17.3	1.6	16.9	17.3	17.8	1

* Extremely warm (EW), very warm (VW), warm (W), normal (N), very cold (VC), extremely cold (EC) ** warm (1), normal (0), cold (−1), categorization RHMZ.

Table 2. Monthly precipitation sums and corresponding percentiles and terciles and their deviations for February, March, April, and May 2024, in Novi Sad (Serbia), compared to the reference period 1991–2020.

Sum (mm)	Perc. Cat. * 1991–2020	Sum (mm) 1991–2020	Deviation from the Average (mm)	1991–2020 33.-Perc.	1991–2020 50.-Perc.	1991–2020 66.-Perc.	Terciles ** Cat.
February							
9.1	D	36.4	−27.3	26.7	39.2	46.8	−1
March							
15.0	D	38.7	−23.7	30.3	36.7	47.8	−1
April							
21.5	D	46.6	−25.1	30.3	43.2	54.0	−1
May							
78.0	N	78.2	−0.2	59.4	74.0	84.8	0

* Extremely wet (EW), very wet (VW), wet (W), normal (N), dry (D), very dry (VD), extremely dry (ED) ** wet (1), normal (0), dry (−1), categorization RHMZ.

Spearman's correlation coefficients were determined, with a probability of $p < 0.05$, for the reference period 1991–2020 and the research period 2010–2023 for average monthly air temperatures (0.986*) and monthly precipitation amounts (0.881*), while the correlations between average monthly temperatures and monthly precipitation sums were less significant (0.800) and (0.838) for the respective periods. The values marked with * are statistically significant and confirm a strong positive correlation between the analyzed parameters, indicating their increase. The results are in accordance with the findings of Vujović and Todorović [32] and WMO [15]. The significance of deviations of the analyzed parameters from the normal was determined by the Mann–Kendall trend test, only for the increase in average monthly air temperatures in the research period 2010–2023. Although trends were noticeable for other parameters, the Mann–Kendall trend test did not statistically confirm them as significant.

The same climatic parameters were specifically analyzed for the 15 years of research for February, March, April, and May—the months when the phenophase of blooming globe flowering ash was recorded in Novi Sad (Table 3).

Table 3. The correlations of mean monthly air temperatures and total precipitation for February, March, April, and May during the research period (2010–2024) according to the Mann–Kendall trend test.

Climat. Parameter	T_{mean}				∑ Precipitation			
Month / Stat. Parameter	II	III	IV	V	II	III	IV	V
S *	45	17	−13	9	−21	−25	−7	−21
Z	2.18	0.79	−0.59	0.39	−0.99	−1.18	−0.30	−0.99
p	0.002	0.427	0.551	0.692	0.322	0.235	0.766	0.322

* S will be negative for a negative trend, zero for no trend, and positive for an increasing trend.

It has been confirmed that, in the period 2010–2024, only the increase in average monthly temperatures in February is statistically significant. A temperature increase was also observed in March and May, while in May, temperatures showed a decline. Monthly precipitation sums in all four months are lower. However, for the mentioned months and both parameters, statistical significance was not confirmed.

3.2. Phenology and Flowering Patterns

Analysis of phenological characteristics confirmed that the blooming period of the studied linear population of globe flowering ash in the GI of Novi Sad was influenced by climatic parameters over the 15 years of research, given that the 42 monitored trees were in the same micro-locational conditions in a small area. The average duration of the blooming phenophase in the period 2010–2024 was 19 days. The earliest starts of all key blooming phases were recorded in 2024: BF—94, FF—101, and EF—109 DOY. The blooming duration was 16 days, but during the research, the shortest blooming phenophase was in 2012 (11 days), when BF was 120 DOY. The year 2012 was climatically specific for Novi Sad, with a warm January and precipitation within normal limits, while February was the coldest since measurements began, with precipitation significantly above normal and snow cover lasting more than twenty days (RHMZ). The absolute difference between the earliest and latest BF is 26 days, but trend analyses show that over 15 consecutive years, blooming phenological patterns vary under the influence of climatic variables, and the blooming of globe flowering ash begins 11 days earlier and ends 2 days earlier in the research area (Figure 7).

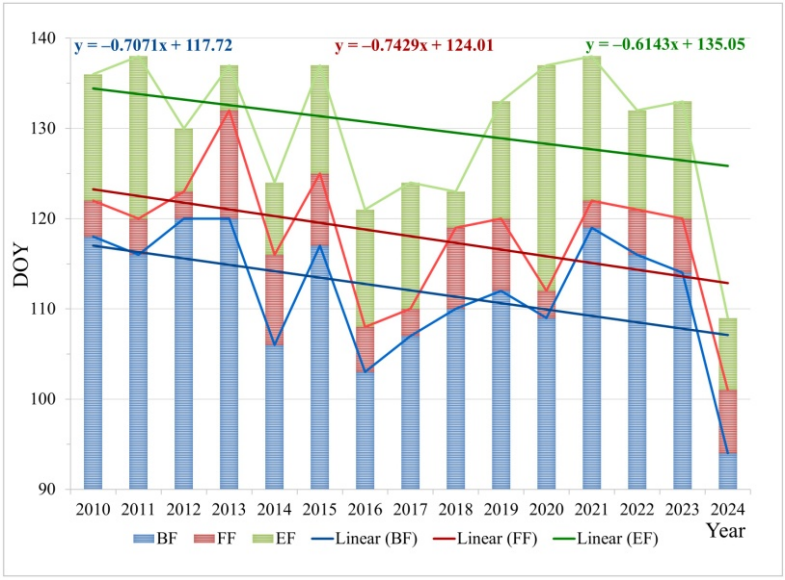

Figure 7. Beginning of flowering (BF), full flowering (FF), and end of flowering (EF) of globe flowering ash and the corresponding linear trends for DOY, in the period 2010–2024 in Novi Sad.

BF was recorded after the accumulation of a heat sum from 358.6 °C (2015, DOY:117) to 462.2 °C (2024, DOY: 94). The average accumulated heat for BF, during the period 2010–2024, was 389.3 °C. FF was recorded after the accumulation of a heat sum from 363.9 °C (2017, DOY:110) to 588.6 °C (2013, DOY: 132). The average accumulated heat for FF, during the period 2010–2024, was 459.2 °C. EF was recorded after the accumulation of a heat sum from 483.5 °C (2017, DOY:124) to 651.6 °C (2020, DOY: 137). The average accumulated heat for EF, during the period 2010–2024, was 587.7 °C. Lower accumulated heat sums in 2017 can be explained by the occurrence of a cold wave, which was the second most intense cold wave after the one recorded in February 2012, while higher sums in 2013 were due to a 12-day heat wave that started in late April and ended in the first decade of May, and in 2020 when there were no cold waves, but a heat wave was recorded in early April and the beginning of the second decade (RHMZ). The determined GDDs during the research period are variable but close regardless of DOY. The linear trends of the blooming phenophase (Figures 7 and 8) confirm that in the blooming pattern, BF, FF, and EF were recorded within certain ranges of accumulated heat. A slight increase in accumulated heat for BF and EF and a slight decrease for FF were observed, which can be explained by

climatic events during the research period, such as the extremely dry April in Novi Sad in 2015, followed by a record daily maximum precipitation in May (RHMZ).

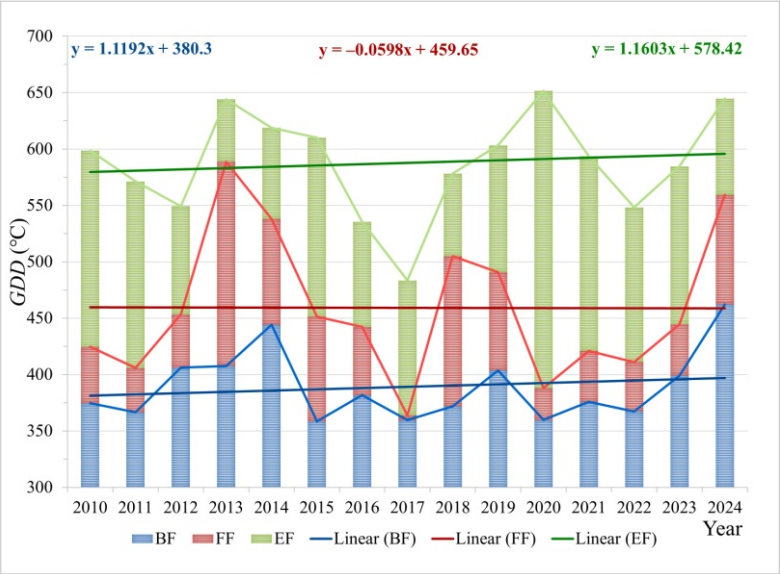

Figure 8. Beginning of flowering (BF), full flowering (FF), and end of flowering (EF) of globe flowering ash and the corresponding linear trends for GDD (°C), in the period 2010–2024 in Novi Sad.

For the assessment of trends, i.e., the impacts of climatic variables on the vulnerability and adaptation of globe flowering ash in the linear planting along the quay in Novi Sad, descriptive statistics were used (Table 4). The average air temperature for the period BF-EF and key elements defines the phenological patterns of blooming, while the standard deviation and other parameters indicate the deviation from the average values and the significance of the shifts in blooming phenophases.

Table 4. Descriptive statistics for average air temperatures during the blooming period (T_{mean} BF-EF) and key events in the blooming phenophase (BF DOY, FF DOY, EF DOY, BF GDD, FF GDD, and EF GDD) of globe flowering ash for the period 2010–2024 in Novi Sad (Serbia).

	T_{mean} (°C) (year)	BF DOY	FF DOY	EF DOY	BF GDD	FF GDD	EF GDD
N	14	15	15	15	15	15	15
Min	11.5	94	101	109	358.6	363.9	483.5
Max	13.9	120	132	138	462.2	588.6	651.6
Sum	177.8	1681	1771	1952	5838.9	6887.5	8815.7
Mean	12.7	112.0667	118.0667	130.1333	389.26	459.1667	587.7133
Std. error	0.177281	1.893514	1.972349	2.155539	8.077888	16.70837	11.82174
Variance	0.44	53.78095	58.35238	69.69524	978.784	4187.545	2096.303
Stand. dev	0.663325	7.33355	7.638873	8.348367	31.28552	64.71125	45.7854
Median	12.7	114	120	133	375.7	444.5	593.7
25 prcntil	12.275	107	112	124	366.7	411	549.3
75 prcntil	13.25	118	122	137	406.1	505	618.8
Kurtosis	−0.18121	1.09291	0.810437	1.377669	0.903862	−0.32039	0.446129
Coeff. var	5.223031	6.543917	6.469966	6.415241	8.037179	14.09319	7.79043

According to [33], phenophases vary depending on local climate, abiotic, and biotic factors, which is why Spearman's correlation coefficients were determined (Figure 9). A maximum positive correlation between BF DOY and FF DOY and a high positive correlation between BF DOY and EF DOY and FF DOY and EF DOY were confirmed. The correlation analysis confirmed that the increase in BF DOY affects the increase in FF DOY and to a lesser extent the increase in FF DOY and EF DOY, indicating the influence of other climatic

variables on the blooming of globe flowering ash. This is further supported by the absence of significant correlations between T_{mean} BF-EF and elements of the blooming phenological patterns. Other correlations were negligible.

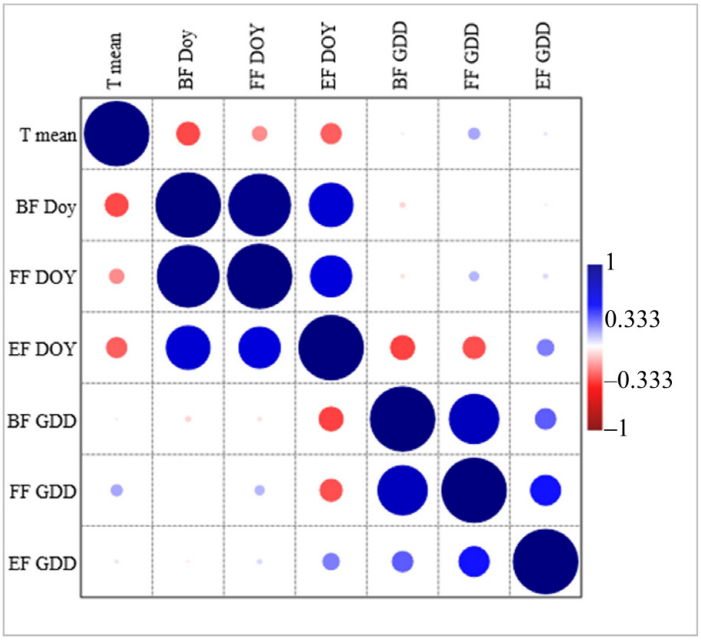

Figure 9. Spearman's correlation coefficients for T_{mean} BF-EF, BF DOY, FF DOY, EF DOY, BF GDD, FF GDD and EF GDD in the period 2010–2023, and BF DOY, FF DOY, EF DOY, BF GDD, FF GDD and EF GDD in the period 2010–2024 for globe flowering ash in Novi Sad (Serbia).

The significance of the deviations of the investigated parameters from the average values was also analyzed using the Mann–Kendall trend test. A statistically significant increasing trend was confirmed only for T_{mean} BF-EF, which is consistent with the findings for average monthly air temperatures during the research years. The trends for other parameters were not statistically significant.

3.3. Morphological Analysis of Compound Inflorescences of Globe Flowering Ash

According to existing literature [34], the length and width of manna ash inflorescences vary from 10 to 20 cm in length and from 8 to 12 cm in width. The analyzed specimens belong to the globe-shaped crown cultivar, and differences in the dimensions of the compound inflorescences compared to the basic species can be observed in addition to habitus differences. The average length of the inflorescences in the analyzed samples was 8.27 cm, while the average width was 9.70 cm, indicating more compact inflorescences in this cultivar compared to the basic species (Table 5). The maximum inflorescence length of 12.00 cm was recorded in individuals numbered 3, 37, and 40, while the minimum length of 4.50 cm was observed in individuals 13, 21, and 22. The greatest inflorescence width of 16.00 cm was noted in individual 5, while the smallest width of 5.50 cm was observed in individuals 4 and 38. The average number of flower clusters was 4.53, with the number of clusters ranging from 3 to 8 per inflorescence. Among the four analyzed morphometric characteristics (inflorescence length and width, number of flower clusters, and number of stamens), the number of stamens showed the greatest variability (CV. 28.67%), confirmed by the large difference between the minimum (180) and maximum (700) number of stamens. Significant variability was also shown in the number of flower clusters, while the length and width of inflorescences had moderate variability.

Duncan's test recorded significant differences and grouping of genotypes of globe flowering ash (Table 5) at $p < 0.05$.

The results of descriptive statistics for the measured parameters of compound inflorescences and ANOVA analysis are presented (Supplementary Table S2), where statistically significant differences at the population level were recorded for the parameters number of flower clusters and number of stamens ($p < 0.05$).

Table 5. Mean values of the measured inflorescence globe flower ash parameters at the genotype level and the results of Duncan's test.

Genotypes	IL *	IW	NFC	NS
1.	9.06 $^{g–m}$ **	12.52 $^{k–n}$	6.60 ^{k}	628.1 ^{r}
2.	9.38 $^{i–n}$	10.69 $^{g–n}$	6.60 $^{g–j}$	583.6 ^{pr}
3.	9.63 $^{k–n}$	11.00 ^{ij}	6.60 $^{f–i}$	624.4 ^{r}
4.	8.70 $^{g–k}$	10.13 $^{f–n}$	6.60 $^{a–g}$	498.3 ^{mno}
5.	9.43 $^{j–n}$	11.39 ^{j}	4.90 $^{e–i}$	537.2 ^{op}
6.	8.78 $^{g–l}$	8.80 $^{a–f}$	4.00 ^{bcd}	507.8 ^{mno}
7.	7.07 ^{abc}	7.70 ^{abc}	3.80 ^{abc}	403.3 $^{g–k}$
8.	9.98 ^{mn}	9.63 $^{d–l}$	4.40 $^{b–i}$	500.2 ^{mno}
9.	8.23 ^{efg}	10.21 $^{f–l}$	4.60 $^{c–i}$	502.7 ^{mno}
10.	8.66 $^{g–j}$	10.34 $^{f–j}$	4.10 $^{a–e}$	513.6 ^{no}
11.	8.53 $^{g–j}$	9.12 $^{a–l}$	3.70 ^{ab}	428.5 $^{i–l}$
12.	9.19 $^{h–n}$	10.29 $^{f–j}$	4.60 $^{c–i}$	415.5 $^{h–k}$
13.	6.21 ^{a}	9.27 $^{b–h}$	4.50 $^{b–i}$	405.5 $^{g–k}$
14.	8.46 ^{ghi}	9.48 $^{d–m}$	4.60 $^{c–i}$	416.2 $^{h–k}$
15.	10.04 ^{n}	11.73 ^{n}	5.30 ^{ij}	482 $^{l–o}$
16.	7.36 ^{cde}	8.77 $^{a–m}$	4.30 $^{a–g}$	385.4 $^{e–j}$
17.	9.65 ^{lmn}	12.20 ^{n}	5.80 ^{j}	588.2 ^{pr}
18.	8.31 ^{fgh}	9.03 $^{a–g}$	4.70 $^{d–i}$	424.8 $^{i–l}$
19.	6.59 ^{abc}	7.63 ^{ab}	4.00 $^{a–d}$	326.1 ^{cde}
20.	8.13 $^{d–g}$	9.56 $^{d–i}$	5.00 $^{f–i}$	446.4 $^{j–m}$
21.	6.20 ^{a}	8.10 $^{a–d}$	4.30 $^{a–g}$	387.3 $^{e–j}$
22.	6.94 ^{abc}	10.04 $^{f–m}$	5.20 ^{hij}	542.8 ^{op}
23.	7.28 ^{bcd}	10.77 $^{h–m}$	5.20 ^{hij}	520 ^{no}
24.	8.70 $^{g–k}$	11.00 ^{ij}	4.70 $^{d–i}$	423 $^{i–l}$
25.	7.50 $^{c–f}$	9.78 $^{d–j}$	4.60 $^{c–i}$	414 $^{g–k}$
26.	7.45 $^{c–f}$	9.10 $^{a–h}$	4.60 $^{c–i}$	414 $^{g–k}$
27.	7.33 $^{b–e}$	8.84 $^{a–f}$	4.00 $^{a–d}$	280 ^{bc}
28.	8.43 ^{gh}	9.76 $^{d–m}$	3.80 ^{abc}	228 ^{ab}
29.	7.10 ^{bc}	10.73 ^{hij}	3.80 ^{abc}	380 $^{e–i}$
30.	7.50 $^{c–f}$	9.73 $^{d–i}$	4.80 $^{d–i}$	480 $^{l–o}$
31.	9.43 $^{j–n}$	9.53 $^{d–i}$	4.20 $^{a–f}$	378 $^{e–i}$
32.	7.40 ^{cde}	8.88 $^{a–f}$	4.40 $^{b–i}$	396 $^{f–k}$
33.	8.57 $^{g–j}$	8.95 $^{a–f}$	5.20 ^{hij}	520 ^{no}
34.	8.75 $^{g–l}$	8.91 $^{a–f}$	3.50 ^{a}	210 ^{a}
35.	9.75 ^{mn}	10.03 $^{f–j}$	5.00 $^{f–i}$	350 $^{d–g}$
36.	9.47 $^{j–n}$	9.80 $^{e–j}$	3.70 ^{ab}	222 ^{a}
37.	9.40 $^{i–n}$	8.99 $^{a–f}$	4.60 $^{c–i}$	460 $^{k–n}$
38.	6.45 ^{ab}	7.54 ^{a}	4.20 $^{a–f}$	314 ^{cd}
39.	9.18 $^{h–n}$	9.32 $^{c–m}$	3.70 ^{ab}	222 ^{ab}
40.	9.96 ^{mn}	11.75 ^{n}	4.80 $^{d–h}$	336 $^{c–f}$
41.	6.60 ^{abc}	8.25 $^{a–e}$	4.30 $^{a–g}$	300 ^{cd}
42.	6.76 ^{abc}	8.24 $^{a–e}$	4.50 $^{b–h}$	356 $^{d–h}$

* Abbreviations: Inflorescence length-IL; Inflorescence width-IW; Number of flower clusters-NFC; Number of stamens-NS. ** Means followed by different letters differ significantly, based on Duncan's test at $p < 0.05$.

Multivariate cluster analysis indicates the separation of globe flowering ash genotypes into two subclusters (Figure 10). The majority of genotypes are grouped in the first subcluster, while the second subcluster includes genotypes 19, 40, 35, 42, 27, 38, 41, 28, 36, 39, and 34. The first subcluster comprises four subgroups with genotypes having similar values of

morphological characteristics of the inflorescences. The subgroup containing genotypes 1, 3, 2, and 17 is characterized by similar values for inflorescence length and number of flower clusters. The inflorescence length in grouped genotypes ranges from 9.06 to 9.65 cm, with a more uniform number of clusters. Genotypes 1, 2, and 3 have the same average values for the number of flower clusters (6.6), while genotype 17 has a slightly lower number of flower clusters (5.8). Genotypes of globe flowering ash numbered 4, 8, 9, 6, 10, 23, 33, 5, 22, 15, 30, 20, and 37 constitute the second hierarchical level within the first subcluster. At a lower level, genotypes 4, 6, 8, 9, and 10 are connected with similar average values for inflorescence length, ranging from 8.23 to 9.98 cm, and a similar average number of stamens (ranging from 498 to 513). Genotypes 5, 22, 23, 30, and 33 form the next group connected by similar average values for the number of flower clusters and the number of stamens. In the subgroup consisting of genotypes 15, 20, 30, and 37, a connection at a low hierarchical level is observed with average values for inflorescence length (7.50 to 10.04 cm) and the number of clusters (4.6 to 5.3). The next group of seven genotypes (7, 13, 32, 16, 21, 29, 31) forms a separate subgroup within the first subcluster, connecting the mentioned genotypes with close average values for inflorescence length (6.20 to 9.43 cm), inflorescence width (7.70 to 10.73 cm), and the number of flower clusters (3.8 to 4.4). Notably, genotypes 7 and 13 are close in average values for the number of stamens (403 and 405). The fourth subgroup within the first subcluster includes genotypes 11, 18, 24, 12, 14, 25, and 26. The subgroup with close values for inflorescence length, width, and number of flower clusters is defined by dendrogram analysis for genotypes 11, 18, 24, 12, and 14, while genotypes 25 and 26 have similar average values for all measured parameters.

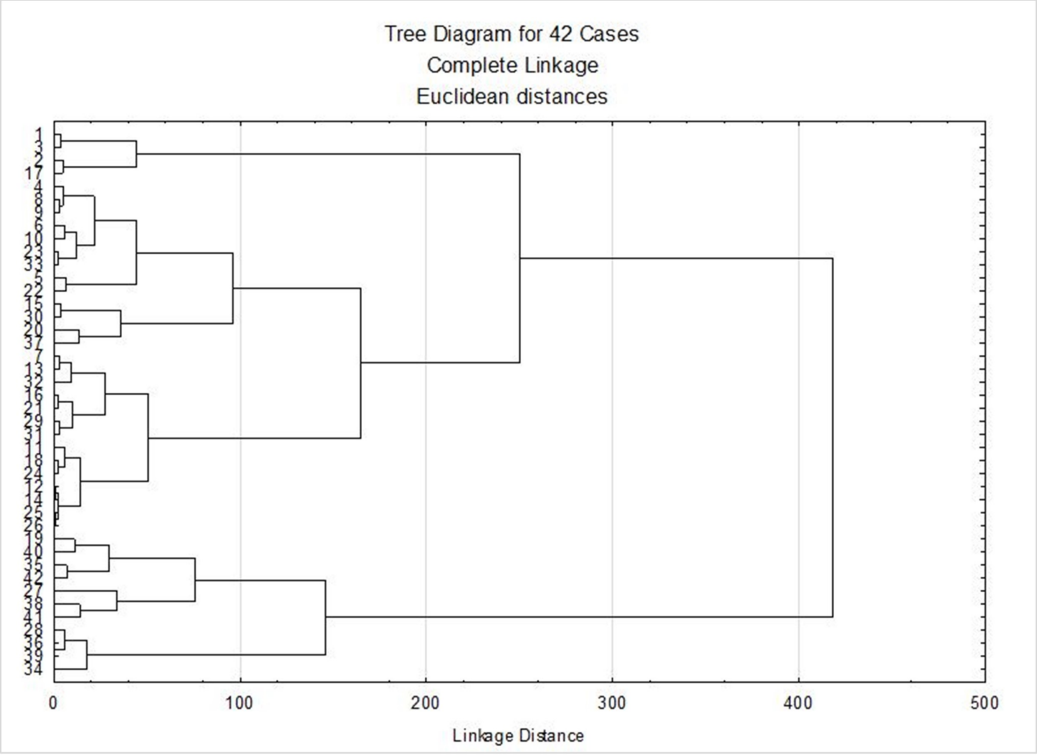

Figure 10. Dendrogram cluster analysis of measured inflorescence parameters of 42 trees globe flower ash genotypes.

The second subcluster identifies three significant groups of globe-flowering ash trees. The first includes genotypes 28, 36, 39, and 34, which can be characterized by similar average values for the number of flower clusters (3.8 to 4.4) and the number of stamens (210 to 228). The second subgroup within this subcluster indicates genotypes close in inflorescence width and number of flower clusters, while the third subgroup comprises genotypes 19, 40, 35, and 42 with similar values for the average number of stamens.

Based on the results of cluster analysis, it was established that the grouping is not conditioned by micro-locational conditions, as even distant individuals showed close values of the measured morphological parameters of inflorescences. It is assumed that the differences are conditioned by genetic dispositions and the origin of the vegetative material used for the propagation of the individuals, considering that the seedlings were grafted.

4. Discussion

The research encompasses the observation of the phenological blooming phases of 42 globe-shaped manna ash trees over a 15-year period, located in a linear planting near a large river flow in the urban core. The objectives of the research are focused on defining measures for the ecological protection and conservation of *Fraxinus ornus* 'Globosa', ecosystem services, and the sustainability of linear greenery. Determining the condition of valuable cultivars, such as the manna ash cultivar, and the potential for its use in green infrastructure solutions in urban areas is of great significance. The reason for this is the rapid growth of cities and the increase in gray infrastructure—roads, buildings, parking lots, etc.—which leads to rising air temperatures and changes in urban ecosystems, negatively affecting the comfort and well-being of residents [35–38]. Therefore, the ecosystem benefits that trees can provide in urban environments are very important. Trees in cities provide many benefits, such as a positive impact on biodiversity conservation, mitigation of climate extremes, carbon sequestration, accumulation of heavy metals, improvement of environmental aesthetics, enhancement of visual perception by giving character to the landscape, as well as providing habitat and food for animals and nectar and pollen for insects [39–42]. Species of the genus *Fraxinus* sp. are an important element of the green infrastructure of cities, especially in street spaces, where they create a better microclimate during summer in urban cores [43]. Based on the financial value of the benefits of woody plant species in cities, the genus *Fraxinus* is among the 10 most valuable genera [44]. Ash trees, due to their compound leaves, stand out as species with a high leaf area index (LAI) and are among the most efficient aerosol depositors, emitting very few biogenic volatile organic compounds (BVOCs) [45]. Due to its ornamental qualities and rounded-elongated habitus, *Fraxinus ornus* L. is often used for greening cities [46]. The manna ash holds a special place in landscape architecture because it is the only species of the genus *Fraxinus* sp. with terminal leaflets and decorative flower clusters, making it very attractive during the blooming phenophase. The tree line of globe manna ash trees in Novi Sad, Serbia, besides providing aesthetic services and regulating microclimate ecological benefits, is an important source of pollen for pollinators. Therefore, the application of the manna ash cultivar in potential spaces for forming green corridors holds an important perspective for the preservation of ecosystem services, forming the foundation for the development of the GI concept and nature-based solutions in urban environments [47].

The period of the beginning of flowering is very important due to the timing of pollination, pollen release, and further generative reproduction of plants. Manna ash flowers do not produce nectar, but they have a pleasant fragrance and attract insects, which are the main pollinators, although pollination can also be anemophilous [10,46,48–50]. Research on the shifts in phenophases of pollination and pollen dispersal represents an important aspect of reproductive success. As a result, the second objective focuses on the impact of climate change on linear planting, by comparing phenological flowering patterns with climatic elements. Experimental research on white ash (*Fraxinus excelsior* L.) conducted by Bochenek and Eriksen [51] showed significant temporal advancement of pollination and the relationship between the phenological advancement of pollen carriers and the reproductive success of their male parent. Urban conditions accelerate the occurrence of phenological phases in ornamental species in cities [52]. Manna ash belongs to the woody species that bloom in late spring. According to the literature, the phenophases of blooming and leafing occur simultaneously, in May [46,49,53]. However, based on our research during the period 2010–2024, the manna ash cultivar had its full blooming phenophase in April, which is a month earlier. Slobodník et al. [54] note that during their research on

the blooming phenophase from 2015 to 2019, they found that blooming in central Slovakia occurred two weeks later than in the southern range of the species. The start of blooming, which is associated with pollen release, occurred between 111 and 139 DOY, depending on the location, which is 7 days later for the earliest DOY (94) and 19 days later for the latest DOY (120) compared to our data. Late spring frosts can damage the flowers of white (*Fraxinus excelsior* L.) and field ash (*Fraxinus angustifolia* Vahl), leading to branch bifurcation and irregular tree growth because they are physiologically active and bloom in early spring. However, since manna ash blooms in late spring, late spring frosts do not pose a threat, as confirmed by our research. Therefore, the application of white (*Fraxinus excelsior* L.) and field ash (*Fraxinus angustifolia* Vahl) is limited due to climate change, as they show frost sensitivity, while manna ash can have broader applications [55].

Regarding the third objective—the determination of the sex of selected trees and the morphometric characteristics of the inflorescences, manna ash represents an androdioecious species, having hermaphroditic flowers or only male flowers with stamens, thus behaving as male plants [46,56]. This is a rare breeding system [57]. The globe flowering ash individuals in our research have only male flowers with stamens and do not produce fruits. The flowers of manna ash form dense panicle inflorescences, 10–20 cm long. The corolla color is creamy white (defined by the RGB color system as 255/255/236) with four linear corolla lobes, each 6 mm long [34]. The inflorescences appear terminally on current-year shoots, along with leafing [58]. This author also noted that due to the exceptionally large inflorescences and the presence of corolla lobes, manna ash is called "flowering ash", and in this species, the inflorescences are a decorative element. For this reason, research on the morphometric characteristics of manna ash inflorescences is important for the visual perception of the urban landscape. According to our research, the globe flowering ash individuals had average values for inflorescence length and inflorescence width, which slightly deviates the from literature data. Given that this is a round-crowned cultivar, it typically forms more compact inflorescences compared to the inflorescences of the basic species, with the ratio of inflorescence length to width (IL/IW) being less than 1.

However, certain populations in Slovakia had the earliest autumn phases and the shortest growing season during the years of research, with only two years (2015 and 2018) marked as years of full yield [54]. Species of the genus *Fraxinus* sp. typically have abundant blooming and fruiting every 2–3 years. These data align with our research, as it was established during 15 years of observation that the examined clones of globe flowering ash trees exhibited alternating blooming intensity, with exceptionally abundant blooming occurring at intervals of 3 years. The studied trees bear only male flowers, and thus fruiting is absent. A characteristic of manna ash is that due to insect pollination, one-third of the seeds on the same tree share the same genetic material as the paternal tree (which reduces genetic diversity). This is not the case with white (*Fraxinus excelsior* L.) and field ash (*Fraxinus angustifolia* Vahl), as they are wind-pollinated and rarely share material with the paternal tree [55]. Male manna ash trees have better reproductive function, more abundant blooming, and better quality pollen material than hermaphroditic trees, which is consistent with our observations of blooming and its abundance. Additionally, seedlings derived from seeds pollinated by male trees have better growth. These findings are expected because hermaphroditic trees expend more resources on creating embryos, fruits, and seeds. Regarding the period of blooming and leafing, both male and hermaphroditic trees had phenophases at the same time. In our research, where only male globe flowering ash trees were recorded, the start of blooming coincided with the onset of leafing, i.e., the appearance of the first leaves. FRAXIGEN [55] confirmed strong blooming synchronization between the sexes, enabling successful pollination between male and hermaphroditic trees.

Fraxinus ornus L. is a fast-growing and pioneer species. Due to its plasticity and rapid germination, it is highly adaptive and easily colonizes new habitats. It is a biomeliorative species, suitable for soil stabilization and reforestation of degraded habitats [46,50,59]. Škvarenina et al. [60] and Machar et al. [61] predict that characteristic broadleaf forests of Europe will shift to higher altitudes in the future due to a lack of moisture and increased air

temperatures. As a thermophilic species, manna ash is very tolerant of high air temperatures and water scarcity, and it is not threatened by a reduction in its range. According to Slobodník et al. [54], due to climate change and spontaneous expansion, manna ash shows traits of range expansion. Despite the latest phenophases and the shortest growing season, manna ash did not show vulnerability but rather great adaptability and potential for expansion. In Serbia, manna ash extends to the northern parts of the country, where it was researched and observed, while the northernmost boundaries of this taxon's range are in Hungary and Slovakia [53].

According to FRAXIGEN [54] none of the three ash species native to Europe (*F. ornus* L., *F. excelsior* L., and *F. angustifolia* Vahl) are endangered or require special conservation programs. However, in recent years, species from the genus *Fraxinus* sp. are not recommended for planting in Canada and North America, and are on the trade prohibition lists in the UK, due to pathogenic insects (*Anoplophora glabripennis* and *Agrilus planipennis*), which can destroy a tree within 2–3 years [59,62,63]. *Agrilus planipennis* most commonly attacks *F. pennsylvanica* Marshall, but attacks on *F. ornus* L. have also been recorded in European Russia [64,65]. These pathogens have not yet been recorded in Serbia, but they are on the Lists of harmful organisms and the lists of plants, plant products, and regulated articles whose introduction and spread in the Republic of Serbia are prohibited [66].

5. Conclusions

The focus of the research was on changes in blooming phenological patterns under the influence of climatic elements. Based on the results of this study, the excellent condition of the globe flowering ash has been established, which could serve as a significant foundation for the future application of this taxon in GI solutions. The globe flowering ash, according to the blooming analysis at the researched locations, did not exhibit vulnerability but demonstrated successful adaptability within the GI of Novi Sad. During the research period, the genotypes of globe flowering ash bloomed every year with moderate to strong intensity during April, with an average blooming duration of 19 days. It was determined that the occurrence of blooming phenological phases of globe flowering ash varied under the influence of climatic variables, with the greatest difference between the earliest and latest BF being 26 days. The analysis of trends in the phenological patterns of the globe flowering ash over 15 consecutive years shows that flowering begins 11 days earlier and ends 2 days earlier in the research area. The earliest start, along with other key phases, was recorded in 2024: BF—94, FF—101, and EF—109 DOY. The calculated GDD for the same phases of the flowering phenological pattern varied but remained within certain ranges of accumulated heat, as confirmed by linear trends. A slight increase in accumulated heat for the start and end phases, and a slight decrease for full flowering, was observed. This is explained by climate events during the months when the flowering phenophases were active, such as drought, heavy rainfall, heat waves, and cold waves. The maximum positive correlations between the days of the year for the flowering phases and the absence of significant correlations with accumulated heat and mean daily air temperatures during the flowering period, in relation to the elements of the flowering phenological patterns, confirm that the flowering phases occur within specific ranges of accumulated heat, independent of DOY. Furthermore, the 2024 year stands out due to exceptionally high air temperatures during the winter and spring periods, with heat waves in February, March, and April.

At the observed location, the genotypes bear male flowers, with more compact inflorescences compared to the basic species, with a high intensity of blooming. The morphometric characteristics of the inflorescences distinguish the studied genotypes of globe flowering ash as a suitable choice for planting in the exceptionally challenging conditions of the urban landscape, aiming to positively influence the visual perception of the urban landscape. The examined secondary populations of globe flowering ash have shown exceptional adaptation to climate change, making them suitable for application in nature-based solutions for GI.

Supplementary Materials: The following supporting information can be downloaded at https://www.mdpi.com/article/10.3390/su16198404/s1, Table S1. Climatic variables for the reference period 1991–2020, research periods 2010–2023 and January–May 2024, and previous time series 1981–2010, 1971–2000, and 1961–1990, for MMS Rimski Šančevi. Table S2. Descriptive statistics and ANOVA of quantitative parameters at the population level of globe flowering ash.

Author Contributions: Conceptualization, M.O., J.Č., D.P., M.L. and S.D.; methodology, M.O. and D.P.; data curation, D.P. and S.D.; writing—original draft preparation, M.O., D.P. and J.Č.; writing—review and editing, M.L. and T.N.; visualization, D.P. and S.D.; supervision, M.O. All authors have read and agreed to the published version of the manuscript.

Funding: The authors declare that financial support was received for research, authorship, and/or publication of this article. This research was supported by the Ministry of Science, Technological Development and Innovation of the Republic of Serbia, contract nos. 451-03-65/2024-03/200117, 451-03-66/2024-03/200117, and 451-03-65/2024-03/200169. In addition, this manuscript covers one of the research topics conducted by researchers at the Centre of Excellence Agro-Ur-For, Faculty of Agriculture, Novi Sad, supported by the Ministry of Science, Technological Development and Innovations, contract no. 451-03-1524/2023-04/17.

Institutional Review Board Statement: Not applicable.

Informed Consent Statement: Not applicable.

Data Availability Statement: The climatology data are freely available at https://www.hidmet.gov.rs/eng/meteorologija/klimatologija_produkti.php (accessed on 10 May 2024). The data from the Republic Hydrometeorological Service of Serbia, which cannot be published, were accessed multiple times.

Acknowledgments: We acknowledge the Ministry of Science, Technological Development, and Innovation of the Republic of Serbia.

Conflicts of Interest: The authors declare no conflicts of interest.

References

1. Rosenzweig, C.; Solecki, W.; Romero-Lankao, P.; Mehrotra, S.; Dhakal, S.; Bowman, T.; Ibrahim, S. *Climate Change and Cities: Second Assessment Report of the Urban Climate Change Research Network*; Cambridge University Press: Cambridge, UK, 2018.
2. Patarkalashvili, T.K. Urban Forests and Green Spaces of Tbilisi and Ecological Problems of the City. *Ann. Agrar. Sci.* **2017**, *15*, 187–191. [CrossRef]
3. Molla, M. The Value of Urban Green Infrastructure and Its Environmental Response in Urban Ecosystem: A Literature Review. *Int. J. Environ. Sci.* **2015**, *4*, 89–101.
4. Mullaney, J.; Lucke, T.; Trueman, S.J. A Review of Benefits and Challenges in Growing Street Trees in Paved Urban Environments. *Landsc. Urban Plan.* **2015**, *134*, 157–166. [CrossRef]
5. Parreño, M.A.; Alaux, C.; Brunet, J.; Buydens, L.; Filipiak, M.; Henry, M.; Keller, A.; Klein, A.; Kuhlmann, M.; Leroy, C.; et al. Critical links between biodiversity and health in wild bee conservation. *Trends Ecol. Evol.* **2022**, *37*, 309–321. [CrossRef] [PubMed]
6. Ballard, W.; Wilson, B.; Udale-Clarke, S.; Illman, H.; Ashley, T.; Kellagher, R. *The SuDS Manual*; CIRIA C753: London, UK, 2015; p. 968. Available online: https://www.ciria.org/ItemDetail?iProductCode=C753F&Category=FREEPUBS (accessed on 30 March 2024).
7. Zhang, S.; Song, H.; Li, X.; Luo, S. Urban Parks Quality Assessment Using Multi-Dimension Indicators in Chengdu, China. *Land* **2024**, *13*, 86. [CrossRef]
8. Primack, R.B.; Higuchi, H.; Miller-Rushing, A.J. The impact of climate change on cherry trees and other species in Japan. *Biol. Conserv.* **2009**, *142*, 1943–1949. [CrossRef]
9. Kunz, A.; Blanke, M. "60Years on"—Effects of ClimaticChange on Tree Phenology—A CaseStudy Using Pome Fruit. *Horticulturae* **2022**, *8*, 110. [CrossRef]
10. Wallander, E. Systematics of *Fraxinus* (Oleaceae) and Evolution of Dioecy. *Plant Syst. Evol.* **2008**, *273*, 25–49. [CrossRef]
11. Brickell, C.D.; Kelly, A.F.; Schneider, F.; Voss, E.G. International Code of Nomenclature for Cultivated Plants—1980. *Regnum Veg.* **1980**, *104*, 32.
12. Obrknežev, R.; Gačević, R.; Bursać, T.; Grujić, Z.; Jovković, M.; Panjković, A.; Marković, V.; Šešum, M.; Letić, M.; Paunić, M.; et al. *Studija Zaštite Životne Sredine Novog Sada*; Javno preduzeće "Urbanizam" Zavod za urbanizam: Novi Sad, Serbia, 2009.
13. Živković, B.; Nejgerbauer, V.; Tanasijević, Đ.; Miljković, N.; Stojković, L.; Drezgić, P. *Zemljišta Vojvodine*; Institut za Poljoprivredna Istraživanja: Novi Sad, Serbia, 1972.
14. Tomić, Z. *Šumarska Fitocenologija*; Šumarski Fakultet Univerziteta u Beogradu: Beograd, Serbia, 2004; pp. 176–182.

15. WMO. *State of the Global Climate 2021: WMO Provisional Report*; World Meteorological Organization (WMO): Geneva, Switzerland, 2021; p. 47. Available online: https://library.wmo.int/records/item/56300-state-of-the-global-climate-2021 (accessed on 10 December 2023).
16. Republički Hidrometeorološki Zavod Srbije (RHMZ). Available online: https://www.hidmet.gov.rs/ciril/meteorologija/klimatologija_godisnjaci.php (accessed on 10 May 2024).
17. Republički Hidrometeorološki Zavod Srbije (RHMZ). Available online: https://www.ogimet.com/synopsc.phtml.en (accessed on 10 May 2024).
18. Fries, A.; Rollenbeck, R.; Nauß, T.; Peters, T.; Bendix, J. Near Surface Air Humidity in a Megadiverse Andean Mountain Ecosystem of Southern Ecuador and Its Regionalization. *Agric. For. Meteorol.* **2012**, *152*, 17–30. [CrossRef]
19. Koch, E.; Bruns, E.; Chmielewski, F.M.; Defila, C.; Lipa, W.; Menzel, A. Guidelines for Plant Phenological Observations. Available online: https://www.researchgate.net/publication/266211199 (accessed on 1 January 2010).
20. Meier, U. (Ed.) *BBCH-Monograph. Growth Stages of Plants. Entwicklungsstadien von Pflanzen. Estadios de las Plantas. Stades de Développement des Plantes*; Blackwell Wissenschafts-Verlag: Berlin, Germany, 1997; p. 622.
21. Buttler, K.P.; Schmid, W. (Eds.) *Anleitung für die phänologischen Beobachter des Deutschen Wetterdienstes*, 3rd ed.; Deutscher Wetterdienst: Offenbach am Main, Germany, 1991.
22. Lalić, B.; Ejcinger, J.; Dalamarta, A.; Orlandini, S.; Firanj Sremac, A.; Paher, B. *Meteorologija i klimatologija za agronome*; Univerzitet u Novom Sadu-Poljoprivredni fakultet: Novi Sad, Serbia, 2021; p. 219.
23. WMO. *Guidelines for Plant Phenological Observations*; WMO/TD No. 1484; 2009. Available online: https://library.wmo.int/records/item/51138-guidelines-for-plant-phenological-observations (accessed on 20 December 2023).
24. McMaster, G.S.; Wilhelm, W.W. Growing degree-days: One equation, two interpretations. *Agric. For. Meteorol.* **1997**, *87*, 291–300. [CrossRef]
25. Gilbert, R.O. *Statistical Methods for Environmental Pollution Monitoring*; Van Nostrand Reinhold: New York, NY, USA, 1987.
26. RHMZ. Available online: https://www.hidmet.gov.rs/data/klimatologija/ciril/zima.pdf (accessed on 18 June 2024).
27. RHMZ. Available online: https://www.hidmet.gov.rs/data/klimatologija/ciril/prolece.pdf (accessed on 18 June 2024).
28. RHMZ. Available online: https://www.hidmet.gov.rs/data/klimatologija/ciril/leto.pdf (accessed on 18 June 2024).
29. RHMZ. Available online: https://www.hidmet.gov.rs/data/klimatologija/ciril/jesen.pdf (accessed on 18 June 2024).
30. IPCC. *Climate Change and Land: An IPCC Special Report on Climate Change, Desertification, Land Degradation, Sustainable Land Management, Food Security, and Greenhouse Gas Fluxes in Terrestrial Ecosystems*; Shukla, P.R., Skea, J., Calvo Buendia, E., Masson-Delmotte, V., Pörtner, H.-O., Roberts, D.C., Zhai, P., Slade, R., Connors, S., van Diemen, R., et al., Eds.; Cambridge University Press: Cambridge, UK; New York, NY, USA, 2019.
31. IPCC. *Global Warming of 1.5 °C. An IPCC Special Report on the Impacts of Global Warming of 1.5 °C Above Pre-Industrial Levels and Related Global Greenhouse Gas Emission Pathways, in the Context of Strengthening the Global Response to the Threat of Climate Change, Sustainable Development, and Efforts to Eradicate Poverty*; Masson-Delmotte, V., Zhai, P., Pörtner, H.-O., Roberts, D., Skea, J., Shukla, P.R., Pirani, A., Moufouma-Okia, W., Péan, C., Pidcock, R., et al., Eds.; Cambridge University Press: Cambridge, UK; New York, NY, USA, 2018.
32. Vujović, D.; Todorović, N. Urban/Rural Fog Differences in the Belgrade Area, Serbia. *Theor. Appl. Climatol.* **2019**, *131*, 889–898. [CrossRef]
33. Denny, E.; Gerst, K.L.; Miller-Rushing, A.J.; Tierney, G.L.; Crimmins, T.M.; Enquist, C.A.; Guertin, P.; Rosemartin, A.H.; Schwartz, M.D.; Thomas, K.A.; et al. Standardized Phenology Monitoring Methods to Track Plant and Animal Activity for Science and Resource Management Applications. *Int. J. Biometeorol.* **2014**, *58*, 591–601. [CrossRef] [PubMed]
34. Idžojtić, M. *Dendrologija—Cvijet, Češer, Plod, Sjeme*; Sveučilište u Zagrebu, Šumarski fakultet: Zagreb, Croatia, 2013.
35. Zuo, J.; Zhao, Z.Y. Green Building Research–Current Status and Future Agenda: A Review. *Renew. Sustain. Energy Rev.* **2014**, *30*, 271–281. [CrossRef]
36. Santamouris, M. Cooling the Cities—A Review of Reflective and Green Roof Mitigation Technologies to Fight Heat Island and Improve Comfort in Urban Environments. *Sol. Energy* **2014**, *103*, 682–703. [CrossRef]
37. Li, X.; Zhou, Y.; Asrar, G.R.; Mao, J.; Li, X.; Li, W. Response of Vegetation Phenology to Urbanization in the Conterminous United States. *Glob. Change Biol.* **2016**, *23*, 2818–2830. [CrossRef]
38. Cosmulescu, S.; Stanciu Buican, A.; Ionescu, M. The Influence of Temperature on Phenology of Ornamental Woody Species in Urban Environment. *Sci. Pap. Ser. B Hortic.* **2020**, *64*, 61–67.
39. Burkle, L.A.; Marlin, J.C.; Knight, T.M. Plant-Pollinator Interactions over 120 Years: Loss of Species, Co-Occurrence, and Function. *Science* **2013**, *339*, 1611–1615. [CrossRef]
40. Qiu, J.; Carpenter, S.R.; Booth, E.G.; Motew, M.; Zipper, S.C.; Kucharik, C.J.; Loheide, S.P., II; Turner, M.G. Understanding Relationships among Ecosystem Services across Spatial Scales and over Time. *Environ. Res. Lett.* **2018**, *13*, 054020. [CrossRef]
41. Li, Q.; Zhu, Y.; Zhu, Z. Calculation and Optimization of the Carbon Sink Benefits of Green Space Plants in Residential Areas: A Case Study of Suojin Village in Nanjing. *Sustainability* **2023**, *15*, 607. [CrossRef]
42. Petrov, D.; Ocokoljić, M.; Galečcić, N.; Skočajić, D.; Simović, I. Adaptability of Prunus cerasifera Ehrh. to Climate Changes in Multifunctional Landscape. *Atmosphere* **2024**, *15*, 335. [CrossRef]

43. Armour, T.; Armour, S.; Hargrave, J.; Revell, T. *Cities Alive: Rethinking Green Infrastructure*; Arup: London, UK, 2014. Available online: https://www.arup.com/globalassets/downloads/insights/cities-alive-rethinking-green-infrastructure.pdf (accessed on 20 June 2024).
44. Rogers, K.; Jaluzot, A.; Neilan, C. *Green Benefits in Victoria Business Improvement District: An Analysis of the Benefits of Trees and Other Green Assets in the Victoria Business Improvement District, An i-Tree Eco, CAVAT and G.I. Valuation Study*; 2012. Available online: https://www.itreetools.org/documents/356/VictoriaUK_BID_iTree.pdf (accessed on 20 June 2024).
45. Wróblewska, K.; Jeong, B.R. Effectiveness of Plants and Green Infrastructure Utilization in Ambient Particulate Matter Removal. *Environ. Sci. Eur.* **2021**, *33*, 110. [CrossRef] [PubMed]
46. Caudullo, G.; de Rigo, D. *Fraxinus ornus* in Europe: Distribution, Habitat, Usage and Threats. In *European Atlas of Forest Tree Species*; San-Miguel-Ayanz, J., de Rigo, D., Caudullo, G., Houston Durrant, T., Mauri, A., Eds.; Publ. Off. EU: Luxembourg, 2016; pp. 100–101.
47. Vujičić, D.; Vasiljević, N.; Radić, B.; Tutundžić, A.; Galečić, N.; Skočajić, D.; Ocokoljić, M. Conceptualisation of the Regulatory Framework of Green Infrastructure for Urban Development: Identifying Barriers and Drivers. *Land* **2024**, *13*, 692. [CrossRef]
48. Giovanetti, M.; Aronne, G. Honey Bee Interest in Flowers with Anemophilous Characteristics: First Notes on Handling Time and Routine on *Fraxinus ornus* and *Castanea sativa*. *Bull. Insectology* **2011**, *64*, 77–82.
49. Abbate, L.; Mercati, F.; Di Noto, G.; Heuertz, M.; Carimi, F.; Fatta Del Bosco, S.; Schicchi, R. Genetic Distinctiveness Highlights the Conservation Value of a Sicilian Manna Ash Germplasm Collection Assigned to *Fraxinus angustifolia* (Oleaceae). *Plants* **2020**, *9*, 1035. [CrossRef] [PubMed]
50. Ocokoljić, M.; Petrov, D.J. *Decorative Dendrology [Dekorativna dendrologija]*; Univerzitet u Beogradu-Šumarski Fakultet: Belgrade, Serbia, 2022; p. 409. (In Serbian)
51. Bochenek, G.M.; Eriksen, B. First Come, First Served: Delayed Fertilization Does Not Enhance Pollen Competition in a Wind-Pollinated Tree, *Fraxinus excelsior* L. (Oleaceae). *Int. J. Plant Sci.* **2011**, *172*, 60–69. [CrossRef]
52. Buican Stanciu, A.; Ionescu, M.; Cosmulescu, S.N. The Influence of Urban Conditions on the Phenology of Some Ornamental Species. *Biharean Biol.* **2021**, *15*, 75–79.
53. Slobodník, B.; Šufliarsky, J.; Slobodníková, L.; Škvarenina, J. Changes in the Course of the Spring Generative Phenological Phases in Manna Ash (*Fraxinus ornus* L.) in Dependence on the Air Temperature Conditions. In Proceedings of the Mendel and Bioklimatologie, International Conference, Brno, Czech Republic, 3–5 September 2014; pp. 3–5.
54. Slobodník, B.; Miňová, L.; Rácz, A.; Belčáková, I.; Štefunková, Z. Analysis of Chosen Growth and Reproductive Traits of Manna Ash (*Fraxinus ornus*) with Regards to Its Expansive Properties. *Biosyst. Divers.* **2023**, *31*, 217–221. [CrossRef]
55. FRAXIGEN. *Ash Species in Europe: Biological Characteristics and Practical Guidelines for Sustainable Use*; Oxford Forestry Institute, University of Oxford: Oxford, UK, 2005; p. 128.
56. Dommée, B.; Geslot, A.; Thompson, J.D.; Reille, M.; Denelle, N. Androdioecy in the Entomophilous Tree *Fraxinus ornus* (Oleaceae). *New Phytol.* **1999**, *143*, 419–426. [CrossRef]
57. Pannell, J.R. What Is Functional Androdioecy? *Funct. Ecol.* **2002**, *16*, 858–869. [CrossRef]
58. Wallander, E. Systematics and Floral Evolution in *Fraxinus* (Oleaceae). *Belg. Dendrol.* **2012**, 38–58.
59. Hirons, A.D.; Sjöman, H. *Tree Species Selection for Green Infrastructure: A Guide for Specifiers, Issue 1.3*; Trees & Design Action Group: Exeter, UK, 2019. Available online: https://www.tdag.org.uk/uploads/4/2/8/0/4280686/tdag_treespeciesguidev1.3.pdf (accessed on 24 June 2024).
60. Škvarenina, J.; Kunca, V.; Križová, E.; Tomlain, J. Impact of the climate change on the water balance of altitudinal vegetation zones and changed critical loads in forest ecosystems in Slovakia. *For. J.* **2006**, *52*, 49–59.
61. Machar, I.; Voženílek, V.; Kirchner, K.; Vlčková, V.; Buček, A. Biogeografický model změn klimatických podmínek vegetační stupňovitosti v Česku [Biogeographic Model of Climate Conditions for Vegetation Zones in Czechia]. *Geografie* **2017**, *122*, 64–82. (In Czech) [CrossRef]
62. CWSF Council of Western State Foresters. *Green Infrastructure in the West*; 2017. Available online: https://www.westernforesters.org/sites/default/files/Green%20Infrastructure%20Synthesis,%20Updated%20Cover.pdf (accessed on 24 June 2024).
63. Woodman, B.; Richter, K. *Elmira Green Infrastructure, Project No. 1975*; Natural Resource Solutions Inc.: Waterloo, ON, Canada, 2018. Available online: https://www.woolwich.ca/media/ssjagoki/elmira-green-infrastructure-report.pdf (accessed on 24 June 2024).
64. Baranchikov, Y.; Seraya, L.; Grinash, M. All European Ash Species Are Susceptible to Emerald Ash Borer *Agrilus planipennis* Fairmaire (Coleoptera: Buprestidae)—A Far Eastern Invader. *Sib. J. For. Sci.* **2014**, *6*, 80–85, (In Russian with English Abstract).
65. Orlova-Bienkowskaja, M.J.; Drogvalenko, A.N.; Zabaluev, I.A.; Sazhnev, A.S.; Peregudova, H.Y.; Mazurov, S.G.; Komarov, E.V.; Andrzej, O.; Biekowski, A.O. Current Range of *Agrilus planipennis* Fairmaire, an Alien Pest of Ash Trees, in European Russia and Ukraine. *Ann. For. Sci.* **2020**, *77*, 29. [CrossRef]
66. Pravilnik o listama štetnih organizama i listama bilja, biljnih proizvoda i propisanih objekata. Available online: http://demo.paragraf.rs/demo/combined/Old/t/t2012_03/t03_0379.htm (accessed on 26 June 2024).